MLTS-01

Characteristics of ripple structures revealed from long-term OH airglow images

Jing Li[1](xxlijing@mail.ustc.edu.cn), Tao Li[1], Xiankang Dou[1], Xin Fang[1], Chiao-Yao She[2], Takuji Nakamura[3], Alan Manson[3], Chris Meek[4], Denise Thorsen[5]*

1CAS Key Laboratory of Geospace Environment, School of Earth and Space Sciences, University of Science and Technology of China, Hefei, Anhui, China
2Department of Physics, Colorado State University, Fort Collins, Colorado, USA.
3National Institute of Polar Research, Tachikawa, Tokyo, Japan
4Institute of Space and Atmospheric Studies, University of Saskatchewan, Saskatoon, Canada
5Department of Electrical and Computer Engineering, University of Alaska Fairbanks, Fairbanks, Alaska, USA

Abstract

Using the dataset observed in the mesopause region by an OH all-sky imager at Yucca Ridge Field Station, Colorado (40.7° N, 104.9° W) from 2003 to 2005, we study the characteristics and seasonal variations of ripple structures. Analyzing simultaneous observations of background wind and temperature by a nearby sodium temperature/wind lidar at Fort Collins, Colorado (40.6° N, 105° W) and a Medium Frequency (MF) radar at Platteville, Colorado (40.2° N, 105.8° W), we are able to statistically study the possible relation between ripples and the background atmosphere conditions. Characteristics and seasonal variations of ripples have been presented in detail in this study. In addition, more than half of observed ripples do not advect with background flow, which have higher Richardson number than other ripples advect with background flow. The former ripples are possibly not instability features, but wave structures that are hard to distinguished from the real instability features.

1. Introduction

1.1 What is ripple structures ?

wavecrests : typically 3-10 number
lifetime: less than 45 min (5-20 min)
λ h: 5-15 km

1.2 Sources:

Small-scale ripple structures, observed in OH airglow images, are believed to be induced by either dynamic instability due to large wind shear or convective instability due to super-adiabatic lapse rate.

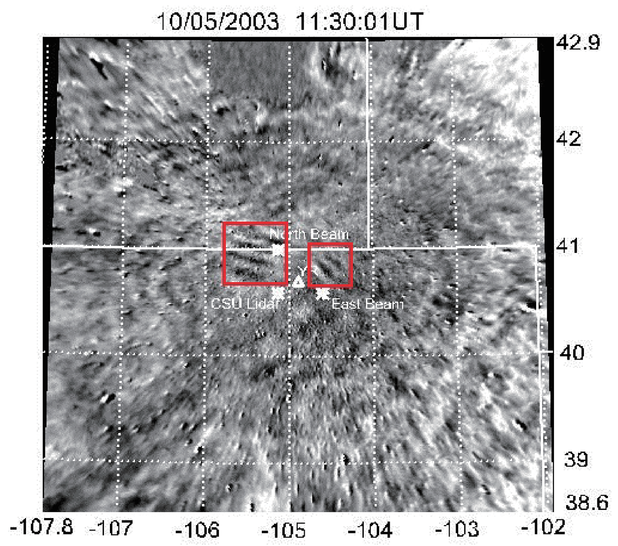

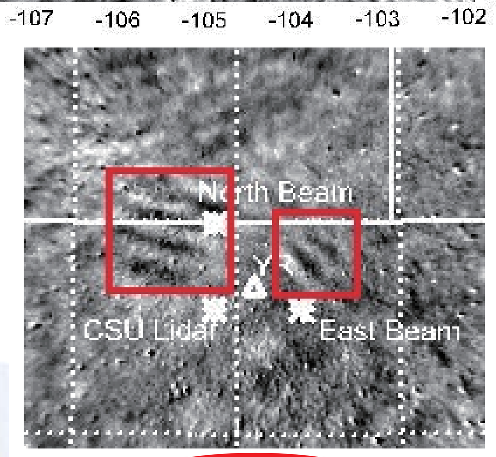

ripple observed by OH airglow images

2. Data and Methods

2.1 Data

All-sky OH imager

Data	Station	Altitude	Temporal resolution	Vertical resolution	Space range
All-sky OH imager	Yucca Ridge Field Station（40.7N, 104.9W）	87±4 km	2 min		500km*500km
CSU Sodium Lidar	Fort Collins, CO（40.6N, 105W）	80-105 km	15 min	2 km	
MF radar	Platteville, CO (40.2°N, 105.8°W)	79-94 km	1hr	3 km	

2.2 Methods

(1) The OH image data is preprocessed , a method of time differencing images to find the possible ripples and calculate the parameters of ripples.
(2) Select days of ripples appear when lidar also works.
(3) Calculating the Squared Brunt-Vaisala frequency (N2) and Richardson number (Ri) to estimate the instabilities when ripples appear.
(4) Comparasion of ripples moving directions and background wind directions.

$$N^2 = \frac{g}{T}\left(\frac{dT}{dz} + \Gamma_d\right)$$

$$Ri = \frac{N^2}{(dU/dz)^2 + (dV/dz)^2} = \frac{N^2}{S}$$

S= (dU/dz)^2+(dV/dz)^2 is the horizontal wind shear.

3. Results and Discussion

3.1 Seasonal Variations and Features

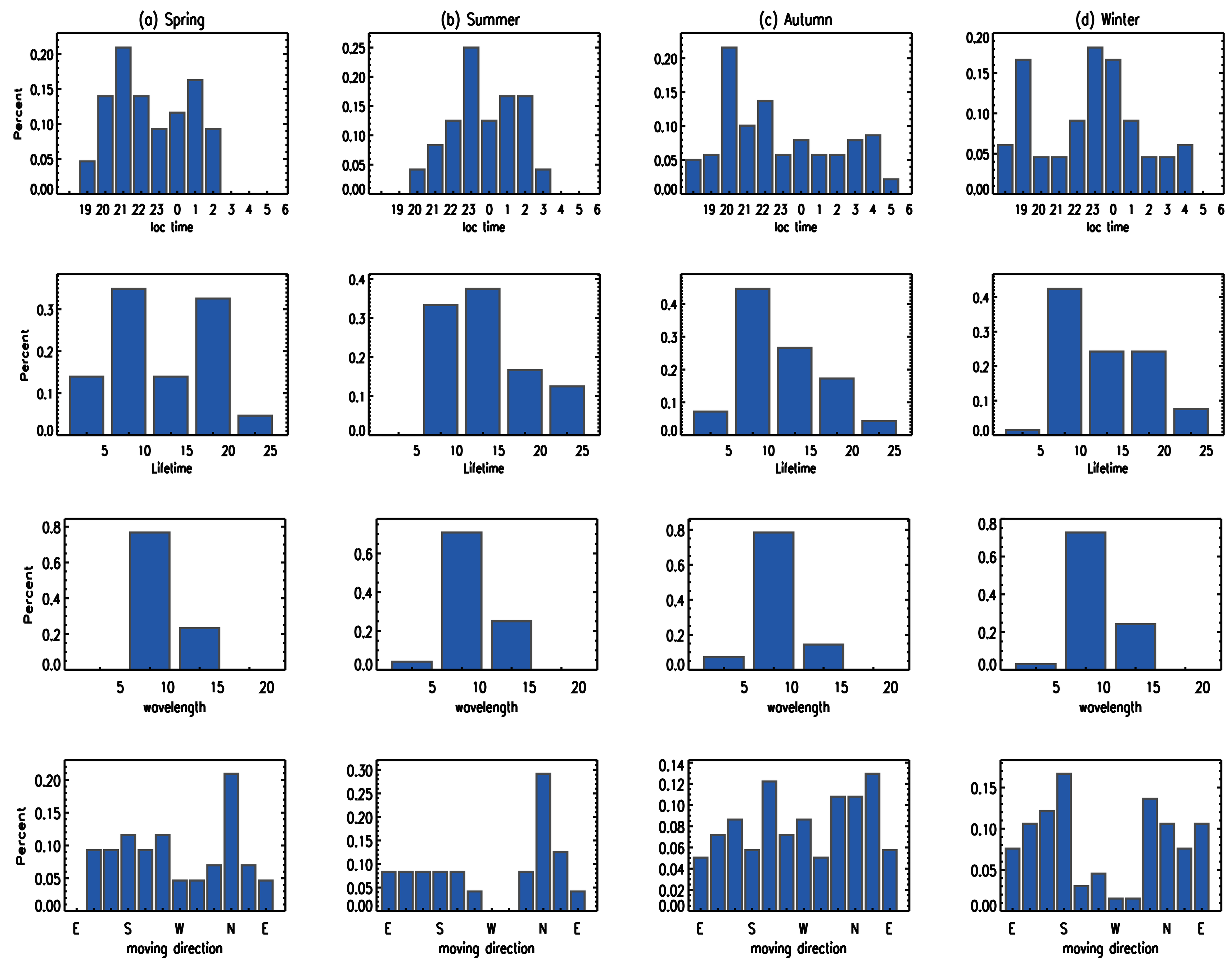

Statistical results of ripples parameters shows that:
(1) ripple occurrence shows local time dependence and seasonal variation.
(2) ripples' lifetime and wavelength are typically 5-20 min and 5-10 km without seasonal variations.
(3) Most of ripples advect toward northward in spring and summer, and toward southward in winter. Seasonal variation of ripples' advection directions is consistent with the seasonal variation of GW propagation direction, which shows a strong northward preference in summer and a southward preference in winter as previously investigated by Dou et al. [2010].

3.2 Correlation between ripples and Instabilities

Figure (a) shows the amount of ripples perpendicular to AGWs is more than those parallel to AGWs. Figure 8(b) reveal that the relation between all ripples and their corresponding instabilities. The probability of instabilities is about 80% with ~60% in dynamic instability.
(1) ripples parallel to AGWs are more likely induced by dynamic instability than those perpendicular to AGWs.
(2) The mesopause atmosphere tends to be unstable When there is a ripple . However, the probability for atmospheric instabilities is lower than ripples occurrence frequency.

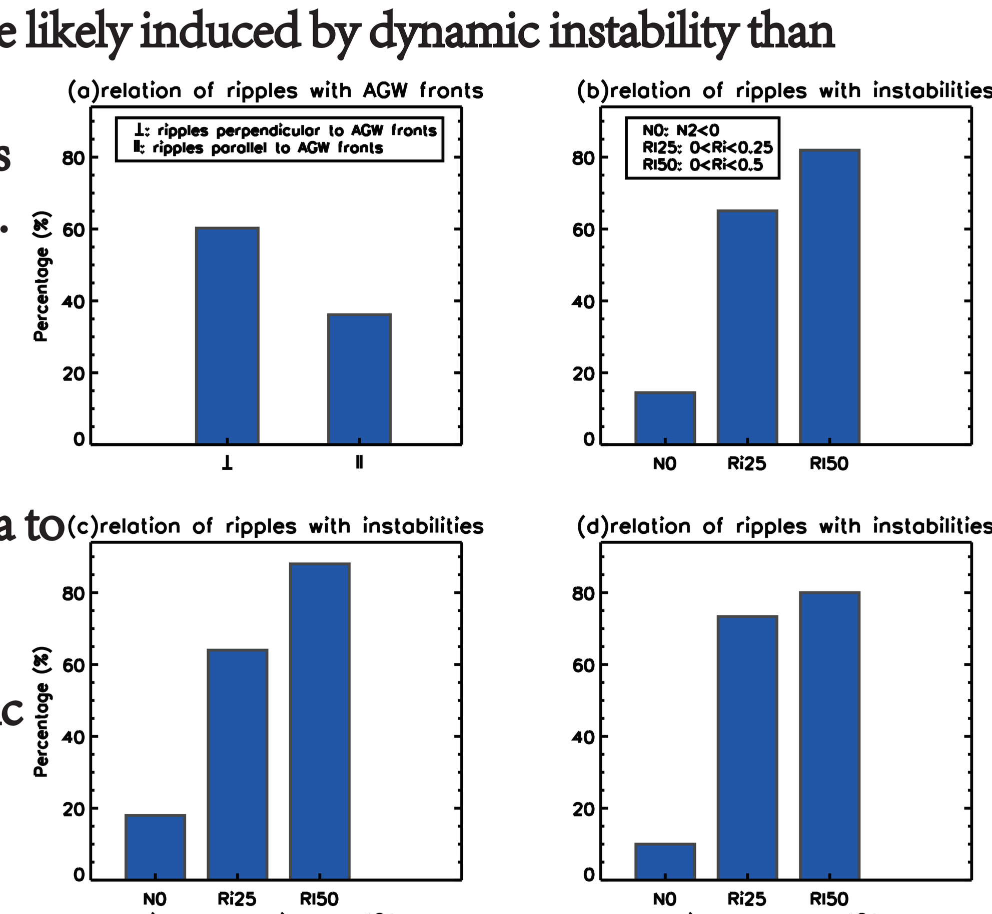

A possible interpretation:
(1) The high sensitivity of imager data to instabilities in OH emission column
(2)Lidar may underestimate the probability of mesopause atmospheric instabilities .
(3) The measurement errors of both the two instruments.
[Hecht et al., 2007]

3.3 Relation between ripples and background winds

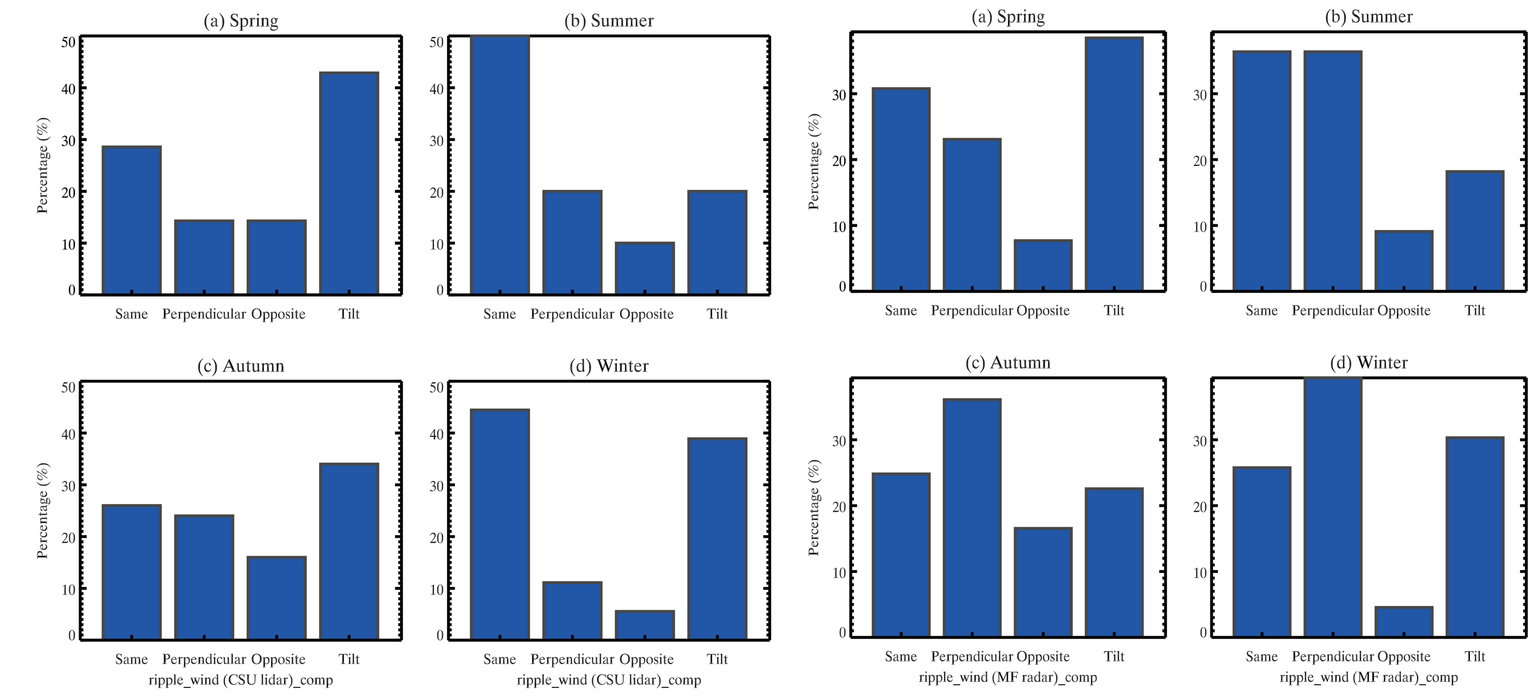

Figures shows that more than half of ripples do not actually advect with background winds, which is different from the previous works[Fritts et al., 1997; Hecht,2004]. These ripples not advect with background winds have much larger speed difference with background winds ,and have higher Ri than other ripples advect with background flow. We still couldn't fully understand why more than half of ripples do not advect with the background winds. However, these ripples are possibly not the instability features; rather, they are wave structures that are hard to distinguished from the real instability features.

4. Conclusion

The major analysis results are as follows:
1. Occurrence frequency of ripples has seasonal variability and local time dependence.
2. The distribution of ripple lifetime, wavelength, advection directions have no clear seasonal variations. The lifetime and spatial scales of these ripples are typically 5-20 min and 5-10 km, respectively. The preferred advection directions of the ripples are either southward or northward.
3. The atmosphere tends to be unstable when ripples occur. However, the probability for atmospheric instabilities is a little lower than ripples occurrence frequency.
4. More than half of ripples do not advect with the background wind, and the Richardson numbers of these ripples are relative higher than others. These ripples are possibly not the instability features, rather wave structures that are hard to distinguished from the real instability features.

Reference

Dou, X. K., T. Li, Y. H. Tang, J. Yue, T. Nakamura, X. H. Xue, B. P. Williams, and C. Y. She (2010), Variability of gravity wave occurrence frequency and propagation direction in the upper mesosphere observed by the OH imager in Northern Colorado, J. Atmos. Sol-terr. Phy, 72(5-6), 457-462, doi:10.1016/j.jastp.2010.01.002.
Fritts, D. C., J. R. Isler, J. H. Hecht, R. L. Walterscheid, and O. Andreassen (1997), Wave breaking signatures in sodium densities and OH nightglow .2. Simulation of wave and instability structures, J. Geophys. Res. Atmos., 102(D6), 6669-6684, doi:10.1029/96jd01902.
Hecht, J. H. (2004), Instability layers and airglow imaging, Rev. Geophys., 42(1), doi:10.1029/2003rg000131.
Hecht, J. H., A. Z. Liu, R. L. Walterscheid, S. J. Franke, R. J. Rudy, M. J. Taylor, and P. D. Pautet (2007), Characteristics of short-period wavelike features near 87 km altitude from airglow and lidar observations over Maui, J. Geophys. Res., 112(D16), doi:10.1029/2006jd008148.

Acknowledgement

The work described in this paper was carried out at the University of Science and Technology of China, under support of the National Natural Science Foundation of China grants (41225017, 41421063, 41304122) and the National Basic Research Program of China grant 2012CB825605.